

Non-Hermitian Chern bands and Chern numbers

Shunyu Yao,¹ Fei Song,¹ and Zhong Wang^{1,2,*}

¹*Institute for Advanced Study, Tsinghua University, Beijing, 100084, China*

²*Collaborative Innovation Center of Quantum Matter, Beijing, 100871, China*

The relation between chiral edge modes and bulk Chern numbers is a paradigmatic example of bulk-boundary correspondence. We show that the Chern numbers defined by a non-Hermitian Bloch Hamiltonian are not strictly tied to the chiral edge modes. This breakdown of correspondence is attributed to the non-Bloch-wave behaviors of non-Hermitian bands. Furthermore, we introduce non-Bloch Chern numbers for non-Hermitian Chern bands, which faithfully count the chiral edge modes. The theory is backed up by the open-boundary energy spectra and dynamics of a representative lattice model, whose phase diagram is found to be consistent with the theoretical prediction. Our results highlight a unique and essential feature of non-Hermitian bands.

Hamiltonians are Hermitian in the standard quantum mechanics. Nevertheless, non-Hermitian Hamiltonians[1, 2] are highly useful in describing many phenomena in nature, such as various open systems[3–12] and waves propagations with gain and loss[13–39]. Recently, topological phenomena in non-Hermitian systems have attracted considerable attentions. For example, it has been proposed that electrons' non-Hermitian self energy stemming from disorder scatterings or e-e interactions[40–42] can generate novel topological effects such as bulk Fermi arcs connecting exceptional points[40, 41] (more recently, this effect has been observed in photonic crystals[43]). The interplay between non-Hermiticity and topology has been a growing field with a host of interesting theoretical[44–74] and experimental[75–81] progresses witnessed in recent years.

A central principle of topological states is the bulk-boundary (or bulk-edge) correspondence, which asserts that the robust boundary states are tied to the bulk topological invariants. Within the band theory, the bulk topological invariants are defined using the Bloch Hamiltonian[82–85]. This has been well understood in the usual context of Hermitian Hamiltonians; nevertheless, it is a subtle issue to generalize this correspondence to non-Hermitian systems[44–52]. As demonstrated numerically[46, 49, 50, 52], the bulk spectra of one-dimensional (1D) open-boundary systems can be remote from those of the corresponding closed systems. Furthermore, through the 1D non-Hermitian Su-Schrieffer-Heeger (SSH) model with a chiral symmetry (Class AIII[84]), it has been shown[52] that topological invariants defined by the Bloch Hamiltonian[45–48] are not strictly related to the zero modes at the ends of an open chain, and a generalized bulk-boundary correspondence enters via the “non-Bloch winding number”[52], which tells the presence or absence of topological end modes.

The topology of the 1D model requires an additional chiral symmetry to stabilize, which is often fragile in real systems. In 2D, Chern bands are robust in the absence of symmetries (i.e., “purely topological”). Non-Hermitian Chern bands are relevant to a number of physical systems (e.g., photonic systems[37], topological-insulator lasers[74, 86]). In an interesting recent work[44], four equivalent Chern numbers (“left/right-left/right”) have been introduced for non-

Hermitian Bloch bands.

In this work, we uncover an unexpected bulk-boundary correspondence of non-Hermitian Chern bands. We find that the chiral edge states are qualitatively different from the predictions by Chern numbers of non-Hermitian Bloch Hamiltonians. This phenomenon is attributed to the non-Bloch-wave character of non-Hermitian bands in the presence of a boundary (edge). Furthermore, we introduce a “non-Bloch Chern number”, which is strictly tied to the number of chiral edge modes. Mathematically, complex-valued wavevector (momentum) is used in its construction, which captures a unique feature of non-Hermitian bands. As an illustration, we study a concrete lattice model, whose energy spectra, dynamics (edge wave propagations), and topological phase diagram is found to be in accordance with our theory.

Bloch Hamiltonian.—We consider a lattice model similar to that of Ref.[44]. The Bloch Hamiltonian is

$$H(\mathbf{k}) = (v_x \sin k_x + i\gamma_x)\sigma_x + (v_y \sin k_y + i\gamma_y)\sigma_y + (m - t_x \cos k_x - t_y \cos k_y + i\gamma_z)\sigma_z, \quad (1)$$

where $\sigma_{x,y,z}$ are Pauli matrices. The Hermitian part is the Qi-Wu-Zhang model[87](a variation of Haldane model[88]); the non-Hermitian parameters $\gamma_{x,y,z}$ appear as “imaginary Zeeman fields”[89]. When $\gamma_{x,y,z} = 0$, the model has a topological transition at $m = t_x + t_y$, where the Chern number jumps. We shall focus on m being close to $t_x + t_y$ ($\gamma_{x,y,z}$ are taken to be small compared to $t_{x,y}$). The eigenvalues of $H(\mathbf{k})$ are

$$E_{\pm}(\mathbf{k}) = \pm \sqrt{\sum_{i=x,y,z} (h_i^2 - \gamma_i^2 + 2i\gamma_i h_i)}, \quad (2)$$

where $(h_x, h_y, h_z) = (v_x \sin k_x, v_y \sin k_y, m - \sum_i t_i \cos k_i)$.

A band is called “gapped” (or “separable”[44]) if its energies in the complex plane are separated from those of other bands. In this model, the Bloch bands are gapped if $E_{\pm}(\mathbf{k}) \neq 0$. The gapped regions are found to be $m > m_+$ and $m < m_-$, where m_{\pm} have simple expressions when $\gamma_z = 0$:

$$m_{\pm} = t_x + t_y \pm \sqrt{\gamma_x^2 + \gamma_y^2}. \quad (3)$$

The Bloch phase boundaries are $m = m_{\pm}$, where the gap-closing point is $\mathbf{k} = (0, 0)$. One can obtain that the $H(\mathbf{k})$ -based Chern number (Bloch Chern number)[44] is 0 for $m > m_+$, 1

for $m < m_-$, and becomes non-definable in the gapless region $m \in [m_-, m_+]$.

Open boundary.—According to the usual bulk-boundary-correspondence scenario, the chiral edge states of an open-boundary system should be determined by the Bloch Chern numbers. Remarkably, our numerical calculations reveal a different physical picture. To be concrete, let us take $\gamma_z = 0$ and focus on the x - y -symmetric cases, namely $v_x = v_y = v$, $t_x = t_y = t$, $\gamma_x = \gamma_y = \gamma$. We fix $v = t = 1$ and solve the real-space lattice Hamiltonian on a square geometry with edge length L in both x and y directions, taking (m, γ) as the varied parameters. We highlight the following findings:

(i) The open-boundary spectra are entirely different from those of Bloch Hamiltonian. Notably, the majority of open-boundary energy eigenvalues are real-valued for the present model with $\gamma_z = 0$, while the Bloch spectra are complex-valued [see Eq.(2)]. This is a sharp difference between these two spectra. Of course, the reality of open-boundary spectra is not a general rule; in other models, it is often the case that both the two spectra are complex (e.g., it is so when γ_z is nonzero); nevertheless, in general these two spectra have pronounced differences.

In addition to the numerical evidence, the reality of square-geometry spectra can be explained as follows. To avoid lengthy notations, we simply take $L = 2$ as an illustration. Let us order the four sites as $(x, y) = (1, 1), (2, 1), (1, 2), (2, 2)$, then the real-space Hamiltonian reads

$$H = \begin{pmatrix} M & T_x & T_y & 0 \\ T_x^\dagger & M & 0 & T_y \\ T_y^\dagger & 0 & M & T_x \\ 0 & T_y^\dagger & T_x^\dagger & M \end{pmatrix} \quad (4)$$

where

$$M = m\sigma_z + i\gamma_x\sigma_x + i\gamma_y\sigma_y, \\ T_x = -\frac{t_x}{2}\sigma_z - i\frac{v_x}{2}\sigma_x, \quad T_y = -\frac{t_y}{2}\sigma_z - i\frac{v_y}{2}\sigma_y. \quad (5)$$

This Hamiltonian is “ η -pseudo-Hermitian”[90, 91] (not PT -symmetric[38, 55]), namely, it satisfies $\eta^{-1}H^\dagger\eta = H$, where η is the direct product of spatial inversion and σ_z :

$$\eta = \begin{pmatrix} 0 & 0 & 0 & \sigma_z \\ 0 & 0 & \sigma_z & 0 \\ 0 & \sigma_z & 0 & 0 \\ \sigma_z & 0 & 0 & 0 \end{pmatrix}. \quad (6)$$

The pseudo-Hermiticity guarantees that from $H|\psi_j\rangle = E_j|\psi_j\rangle$, one can infer $E_j\langle\psi_j|\eta|\psi_j\rangle = E_j^*\langle\psi_j|\eta|\psi_j\rangle$, which means $E_j = E_j^*$ when $\langle\psi_j|\eta|\psi_j\rangle \neq 0$. In this model, we find that the majority of eigenstates have $\langle\psi_j|\eta|\psi_j\rangle \neq 0$.

The distinction between open-boundary and closed-boundary spectra has also been known in a 1D model[46, 49, 50, 52], where the reality of open-boundary spectra becomes most transparent via a similarity transformation, which ensures that the spectra are the same as those of an associated Hermitian Hamiltonian[52]. Such a transformation is absent

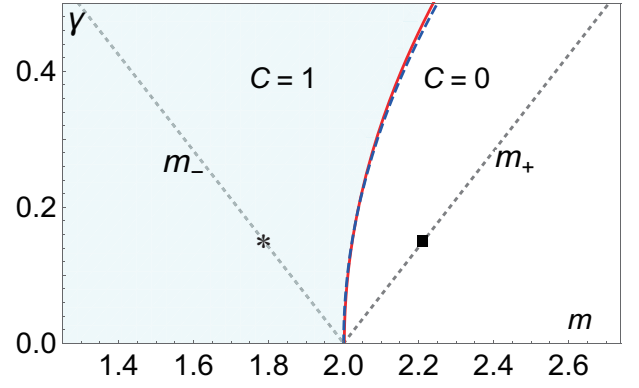


FIG. 1. Topological phase diagram based on the spectra on a square (for $v_{x,y} = t_{x,y} = 1$, $\gamma_{x,y} = \gamma$, $\gamma_z = 0$). Chiral edge states are found in the shadow area, which is therefore topologically nontrivial. The trivial-nontrivial phase boundary (red solid curve) is well approximated by the theoretical curve in Eq.(14) (shown as the blue dashed line, which is very close to the red solid curve). Away from this phase boundary, the spectra of square are gapped. The Bloch-Hamiltonian phase boundaries are shown as the dotted lines, whose equations are $m = m_\pm$ with $m_\pm = 2 \pm \sqrt{2}\gamma$. The Bloch-Hamiltonian spectra are gapless in the fan $m \in [m_-, m_+]$. The non-Bloch Chern number C is defined in Eq.(13) (We take the $E_\alpha < 0$ band and omit the α index; see text).

in the present 2D model, which is therefore a more representative and nontrivial example of open-closed distinction.

(ii) The open-boundary topological phase transitions, where the chiral edge modes are created from or annihilated into the bulk spectra, do not occur at the Bloch phase boundary at $m = m_\pm$ [Eq.(3)]. By numerically scanning the gap-closing points[92], we find that the phase boundary is a single curve (red solid one in Fig.1), in sharp contrast to the two straight lines $m = m_\pm$ obtained from the Bloch Hamiltonian. Furthermore, the numerical phase boundary can be well approximated by the theoretical prediction of Eq.(14).

As an illustration of the phase diagram, we show in Fig. 2 the numerical spectra for two values of parameters indicated as ■ and * in Fig.1. Both ■ and * are taken at the Bloch phase boundary where the Bloch Hamiltonian is gapless. Remarkably, the spectra at ■ clearly display an energy gap ≈ 0.4 . A similar bulk gap is found for the * point; in addition, there are a few in-gap energies, which can be identified as those of chiral edge modes. The absence/existence of chiral edge modes can also be detected by wave packet motions (Fig.2, right panels). In Fig.2(a), there is no chiral edge modes, and the initial wavefunction are superpositions of bulk eigenstates, therefore the wave packet quickly enters the bulk; in Fig.2(b), one can see clear signatures of chiral motions along the edge.

Non-Bloch Chern number.—To understand the underlying physics, let us seek clues in the behaviors of bulk eigenstates. Interestingly, we find that all the bulk eigenstates are localized near a corner of the square[93] (It remains meaningful to talk about “bulk eigenstates” for a large system size because the density of states is proportional to L^2). Furthermore, fo-

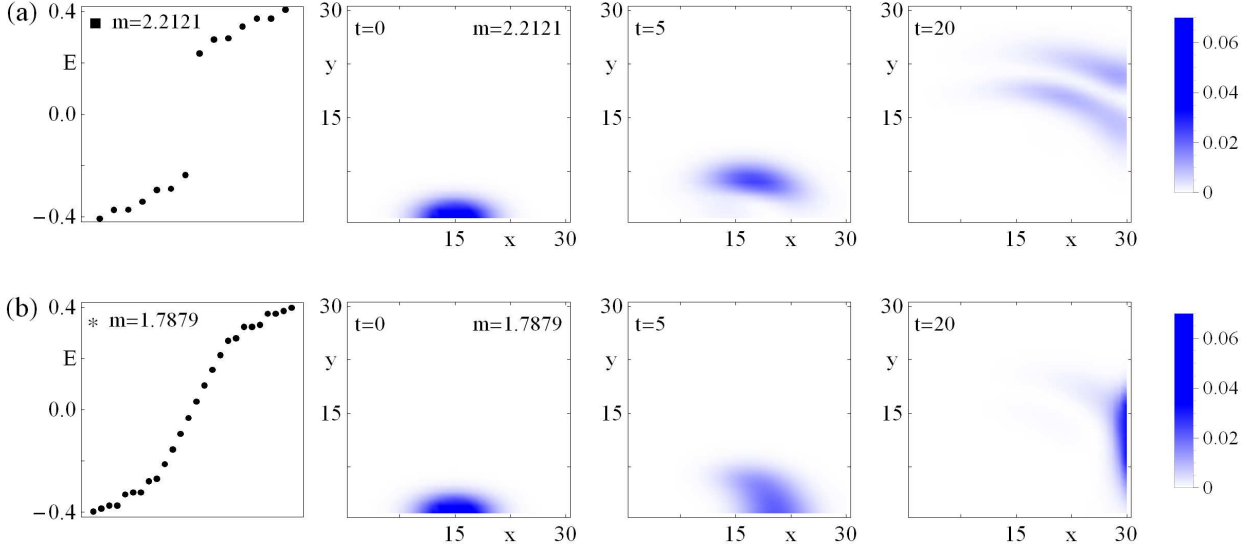


FIG. 2. Lowest energy eigenvalues of a square geometry with $L = 30$ (left panel) and wave-packet evolutions (right three panels). (a) $m = 2.2121$; (b) $m = 1.7879$ (indicated by \blacksquare and $*$ in Fig.1), with $\gamma = 0.15$ for both. The energy eigenvalues shown here are real-valued. In (a), a nonzero energy gap is apparent; in (b), there are a few in-gap energies of chiral edge states. For the wave-packet evolution, the initial wave packet takes the Gaussian form $\psi(t=0) = \mathcal{N} \exp[-(x-15)^2/40 - (y-1)^2/10](1, 1)^T$, \mathcal{N} being the normalization factor, and evolves according to the Schrodinger equation $i\partial_t|\psi(t)\rangle = H|\psi(t)\rangle$. The intensity profile of $|\psi(t)\rangle$ (modulus squared), normalized so that the total intensity is 1, is shown for $t = 0, 5, 20$. The wave packet quickly fades into the bulk in (a), while the chiral (unidirectional) edge motion is appreciable in (b).

cusing on the low-energy bulk eigenstates, we find that their spatial decay can be well fitted by $\exp[(\gamma_x/v_x)x + (\gamma_y/v_y)y]$. Accordingly, these low-energy eigenstates are superpositions of “exponentially-modulated Bloch waves” whose spatial dependence is $\exp[(\gamma_x/v_x)x + (\gamma_y/v_y)y] \exp(i\tilde{k}_x x + i\tilde{k}_y y)$, $\tilde{k}_{x,y}$ being real. Therefore, to describe open-boundary systems, we should take the following replacement in the Bloch Hamiltonian [Eq.(1)]:

$$k_i \rightarrow \tilde{k}_i + i\delta_i(\tilde{\mathbf{k}}) \quad (7)$$

where both \tilde{k}_i and $\delta_i(\tilde{\mathbf{k}})$ are real-valued, and $\delta_i(\tilde{\mathbf{k}})$ takes the simple form $\delta_i = -\gamma_i/v_i$ for small $\tilde{\mathbf{k}}$ in the present model. In other words, the wavevector \mathbf{k} acquires an imaginary part $i\delta(\tilde{\mathbf{k}})$ and becomes complex-valued. The resultant “non-Bloch Hamiltonian” is

$$\tilde{H}(\tilde{\mathbf{k}}) \equiv H(\mathbf{k} \rightarrow \tilde{\mathbf{k}} + i\delta(\tilde{\mathbf{k}})). \quad (8)$$

In the spirit of low-energy theory, we take the continuum limit of Eq.(1) by the substitutions $\sin k_i \rightarrow k_i$ and $\cos k_i \rightarrow 1 - k_i^2/2$:

$$H(\mathbf{k}) = (v_x k_x + i\gamma_x)\sigma_x + (v_y k_y + i\gamma_y)\sigma_y + (m - t_x - t_y + \frac{t_x}{2}k_x^2 + \frac{t_y}{2}k_y^2)\sigma_z, \quad (9)$$

where we have let $\gamma_z = 0$ for simplicity. After the replacement $k_i \rightarrow \tilde{k}_i - i\gamma_i/v_i$ explained above, the “non-Bloch” continuum Hamiltonian is

$$\tilde{H}(\tilde{\mathbf{k}}) = v_x \tilde{k}_x \sigma_x + v_y \tilde{k}_y \sigma_y + (\tilde{m} + \frac{t_x}{2}\tilde{k}_x^2 + \frac{t_y}{2}\tilde{k}_y^2)\sigma_z, \quad (10)$$

where we have discarded a small $-i\sum_{i=x,y} t_i \gamma_i \tilde{k}_i / v_i \sigma_z$ term, which is not important to determining the phase boundary; crucially, we have

$$\tilde{m} = m - t_x - t_y - \frac{t_x \gamma_x^2}{2v_x^2} - \frac{t_y \gamma_y^2}{2v_y^2}. \quad (11)$$

The above approach towards $\tilde{H}(\tilde{\mathbf{k}})$ is quite general and can in principle be implemented directly on lattice models without taking the continuum limit. The general forms of Eq.(7) and Eq.(8) remain applicable.

Our non-Bloch Chern number is defined as the standard Chern number of $\tilde{H}(\tilde{\mathbf{k}})$ (not of $H(\mathbf{k})$ [44]). Since $\tilde{H}(\tilde{\mathbf{k}})$ is generally non-Hermitian, we define the standard right/left eigenvectors by

$$\tilde{H}(\tilde{\mathbf{k}})|u_{R\alpha}\rangle = E_\alpha|u_{R\alpha}\rangle, \quad \tilde{H}^\dagger(\tilde{\mathbf{k}})|u_{L\alpha}\rangle = E_\alpha^*|u_{L\alpha}\rangle, \quad (12)$$

where α is the band index. In fact, one can diagonalize $\tilde{H}(\tilde{\mathbf{k}})$ as $\tilde{H} = T J T^{-1}$, then every column of T (or $(T^\dagger)^{-1}$) is a right (or left) eigenvector, and the normalization $\langle u_{L\alpha} | u_{R\beta} \rangle = \delta_{\alpha\beta}$ is automatically satisfied. This is followed by the standard definition of projection operator: $P_\alpha(\tilde{\mathbf{k}}) = |u_{R\alpha}(\tilde{\mathbf{k}})\rangle\langle u_{L\alpha}(\tilde{\mathbf{k}})|$. We then introduce the non-Bloch Chern number on the generalized Brillouin-zone torus T^2 parameterized by $\tilde{\mathbf{k}}$:

$$C_{(\alpha)} = \frac{1}{2\pi i} \int_{T^2(\tilde{\mathbf{k}})} d^2\tilde{\mathbf{k}} \epsilon^{ij} \text{Tr}(P_\alpha \partial_i P_\alpha \partial_j P_\alpha), \quad (13)$$

which can also be expressed in terms of the Berry curvature. The key in this definition is the “generalized Brillouin zone” parameterized by $\tilde{\mathbf{k}}$ instead of the usual Bloch wavevector \mathbf{k} .

For the present two-band model, the spectra of the continuum $\hat{H}(\tilde{\mathbf{k}})$ in Eq.(10) are real, and we shall focus on the Chern number of the $E_\alpha < 0$ band, omitting the α index in Eq.(13). We compute the Chern number from Eq.(10), and obtain that $C = 1$ (0) for $\tilde{m} < 0$ (> 0). We note that the Chern integrand is well-behaved for $\tilde{\mathbf{k}} \rightarrow \infty$ due to the $\tilde{k}_i^2 \sigma_z$ terms. When $t_{x,y} = v_{x,y} = 1$, $\gamma_{x,y} = \gamma$, the topologically-nontrivial condition $\tilde{m} < 0$ becomes $m < 2 + \gamma^2$, and the phase boundary is

$$m = 2 + \gamma^2, \quad (14)$$

which is confirmed by our numerical calculations (see Fig.1). We note that in the low-energy theory, γ is treated as being small, and we can see from Fig.1 that $\gamma \sim 0.5$ remains well-described by it. As a comparison, the Bloch Chern number[44] is nonzero only when $m < 2 - \sqrt{2}\gamma$; moreover, the Bloch Chern number cannot be defined for $m \in [2 - \sqrt{2}\gamma, 2 + \sqrt{2}\gamma]$ because the bands are gapless.

To summarize our approach: One has to fit or calculate the spatial-decay factors $\delta(\tilde{\mathbf{k}})$ of eigenstates, which are then used to generate $\hat{H}(\tilde{\mathbf{k}})$. The non-Bloch Chern number is then defined via $\hat{H}(\tilde{\mathbf{k}})$ in a standard manner. Working in the low-energy continuum limit is convenient because of the absence of $\tilde{\mathbf{k}}$ dependence of $\delta(\tilde{\mathbf{k}})$. The formulation is conceptually the same if one does not take the continuum limit, though the $\tilde{\mathbf{k}}$ dependence would complicate the fitting or calculations of $\delta(\tilde{\mathbf{k}})$. It will be useful to develop efficient general algorithms to calculate $\delta(\tilde{\mathbf{k}})$ and C in this approach, which is left for future studies.

Cylinder.—Now we briefly discuss the cylinder geometry to clarify some potential confusions. Suppose that the cylinder has periodic-boundary condition in the x direction, and open-boundary condition in the y direction. In this geometry, the spectra can be solved as 1D open-boundary systems along the y direction, with the good quantum number k_x taken as a Hamiltonian parameter. As an illustration, let us take a set of parameters indicated as * in Fig.3(a), and show the numerical spectra in Fig.3(b). Chiral edge states can be readily seen in the spectra.

In fact, to characterize the chiral edge states on the cylinder, one can define a “cylinder Chern number”, which is denoted as C_y because of the open-boundary condition in the y direction. The definition is quite similar to Eq.(13), except that $(\tilde{k}_x, \tilde{k}_y)$ is replaced by (k_x, \tilde{k}_y) , because the eigenstates are forced to be Bloch waves in the x direction. A “cylinder Hamiltonian” $\hat{H}_y(k_x, \tilde{k}_y)$ can be defined in a manner similar to $\hat{H}(\tilde{k}_x, \tilde{k}_y)$, and the cylinder Chern number C_y can be defined based on this “cylinder Hamiltonian”, which we shall not repeat due to the resemblance to the construction of C [Eq.(13)].

We would like to emphasize two points: (i) The cylinder Chern number depends on the edge orientation, namely, if we take open-boundary condition in a different direction, the cylinder Chern number can be different. (ii) The original non-Bloch Chern number defined in Eq.(13) is the physically more relevant one. In fact, we have found that the wave-packet motions on the edges of cylinder still follow the phase diagram of Fig.1, namely, chiral edge motions can be detected

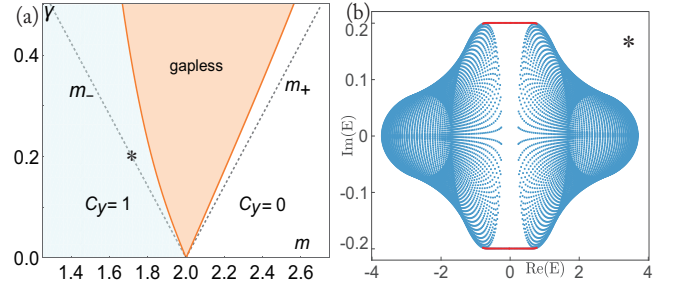


FIG. 3. (a) The “phase diagram” based on the spectra on a cylinder with open boundary condition in the y direction. $t_{x,y} = v_{x,y} = 1$, $\gamma_{x,y} = \gamma$, $\gamma_z = 0$. The dotted lines are the Bloch phase boundaries. (b) The spectra for $(m, \gamma) = (1.717, 0.2)$ (indicated as * in (a)). The length in y direction is $L_y = 40$, and 180 grid points are taken for k_x . The spectra for all k_x 's are shown together in the complex plane, without specifying the k_x value for each data point. The chiral edge states are colored red.

when C (instead of C_y) is nonzero. This phenomenon is understandable because wave packets are quite ignorant of the periodic-boundary condition in the x direction if the cylinder circumference is much larger than the wave packet size in this direction.

Final remarks.—We have introduced a non-Hermitian bulk-boundary correspondence that the chiral edge states are determined by a “non-Bloch” Chern number instead of the usual Bloch Chern numbers. The resultant topological phase diagrams are qualitatively different from the Bloch-Hamiltonian counterparts.

There are many open questions ahead. For example, it is worthwhile to study the respective roles of the Bloch and non-Bloch Chern numbers: What aspects of non-Hermitian physics are described by the Bloch/non-Bloch one? In addition, the theory can be generalized to many other topological non-Hermitian systems. It is also interesting to go beyond the band theory (e.g., to consider interaction effects).

Acknowledgements.—We would like to thank Hui Zhai for discussions. This work is supported by NSFC under grant No. 11674189.

* wangzhongemail@gmail.com

- [1] C. M. Bender, Reports on Progress in Physics **70**, 947 (2007).
- [2] C. M. Bender and S. Boettcher, Physical Review Letters **80**, 5243 (1998).
- [3] I. Rotter, Journal of Physics A: Mathematical and Theoretical **42**, 153001 (2009).
- [4] S. Malzard, C. Poli, and H. Schomerus, Phys. Rev. Lett. **115**, 200402 (2015).
- [5] H. J. Carmichael, Phys. Rev. Lett. **70**, 2273 (1993).
- [6] B. Zhen, C. W. Hsu, Y. Igarashi, L. Lu, I. Kaminer, A. Pick, S.-L. Chua, J. D. Joannopoulos, and M. Soljačić, Nature **525**, 354 (2015).
- [7] S. Diehl, E. Rico, M. A. Baranov, and P. Zoller, Nature Physics **7**, 971 (2011).

- [8] H. Cao and J. Wiersig, *Rev. Mod. Phys.* **87**, 61 (2015).
- [9] Y. Choi, S. Kang, S. Lim, W. Kim, J.-R. Kim, J.-H. Lee, and K. An, *Phys. Rev. Lett.* **104**, 153601 (2010).
- [10] P. San-Jose, J. Cayao, E. Prada, and R. Aguado, *Scientific reports* **6**, 21427 (2016).
- [11] T. E. Lee and C.-K. Chan, *Phys. Rev. X* **4**, 041001 (2014).
- [12] T. E. Lee, F. Reiter, and N. Moiseyev, *Phys. Rev. Lett.* **113**, 250401 (2014).
- [13] K. G. Makris, R. El-Ganainy, D. N. Christodoulides, and Z. H. Musslimani, *Phys. Rev. Lett.* **100**, 103904 (2008).
- [14] S. Longhi, *Phys. Rev. Lett.* **103**, 123601 (2009).
- [15] C. E. Rüter, K. G. Makris, R. El-Ganainy, D. N. Christodoulides, M. Segev, and D. Kip, *Nature physics* **6**, 192 (2010).
- [16] S. Klaiman, U. Günther, and N. Moiseyev, *Phys. Rev. Lett.* **101**, 080402 (2008).
- [17] S. Bittner, B. Dietz, U. Günther, H. L. Harney, M. Miski-Oglu, A. Richter, and F. Schäfer, *Phys. Rev. Lett.* **108**, 024101 (2012).
- [18] A. Regensburger, C. Bersch, M.-A. Miri, G. Onishchukov, D. N. Christodoulides, and U. Peschel, *Nature* **488**, 167 (2012).
- [19] A. Guo, G. J. Salamo, D. Duchesne, R. Morandotti, M. Volatier-Ravat, V. Aimez, G. A. Siviloglou, and D. N. Christodoulides, *Phys. Rev. Lett.* **103**, 093902 (2009).
- [20] M. Liertzer, L. Ge, A. Cerjan, A. D. Stone, H. E. Türeci, and S. Rotter, *Phys. Rev. Lett.* **108**, 173901 (2012).
- [21] B. Peng, Ş. Özdemir, S. Rotter, H. Yilmaz, M. Liertzer, F. Monifi, C. Bender, F. Nori, and L. Yang, *Science* **346**, 328 (2014).
- [22] Z. Lin, H. Ramezani, T. Eichelkraut, T. Kottos, H. Cao, and D. N. Christodoulides, *Phys. Rev. Lett.* **106**, 213901 (2011).
- [23] L. Lu, J. D. Joannopoulos, and M. Soljacic, *Nat Photon* **8**, 821 (2014).
- [24] L. Feng, Y.-L. Xu, W. S. Fegadolli, M.-H. Lu, J. E. Oliveira, V. R. Almeida, Y.-F. Chen, and A. Scherer, *Nature materials* **12**, 108 (2013).
- [25] R. Fleury, D. Sounas, and A. Alù, *Nature communications* **6**, 5905 (2015).
- [26] L. Chang, X. Jiang, S. Hua, C. Yang, J. Wen, L. Jiang, G. Li, G. Wang, and M. Xiao, *Nature photonics* **8**, 524 (2014).
- [27] H. Hodaei, A. U. Hassan, S. Wittek, H. Garcia-Gracia, R. El-Ganainy, D. N. Christodoulides, and M. Khajavikhan, *Nature* **548**, 187 (2017).
- [28] H. Hodaei, M.-A. Miri, M. Heinrich, D. N. Christodoulides, and M. Khajavikhan, *Science* **346**, 975 (2014).
- [29] L. Feng, Z. J. Wong, R.-M. Ma, Y. Wang, and X. Zhang, *Science* **346**, 972 (2014).
- [30] K. Kawabata, Y. Ashida, and M. Ueda, *Phys. Rev. Lett.* **119**, 190401 (2017).
- [31] T. Gao, E. Estrecho, K. Bliokh, T. Liew, M. Fraser, S. Brodbeck, M. Kamp, C. Schneider, S. Höfling, Y. Yamamoto, *et al.*, *Nature* **526**, 554 (2015).
- [32] H. Xu, D. Mason, L. Jiang, and J. Harris, *Nature* **537**, 80 (2016).
- [33] Y. Ashida, S. Furukawa, and M. Ueda, *Nature communications* **8**, 15791 (2017).
- [34] W. Chen, Ş. K. Özdemir, G. Zhao, J. Wiersig, and L. Yang, *Nature* **548**, 192 (2017).
- [35] K. Ding, G. Ma, M. Xiao, Z. Q. Zhang, and C. T. Chan, *Phys. Rev. X* **6**, 021007 (2016).
- [36] C. A. Downing and G. Weick, *Phys. Rev. B* **95**, 125426 (2017).
- [37] T. Ozawa, H. M. Price, A. Amo, N. Goldman, M. Hafezi, L. Lu, M. Rechtsman, D. Schuster, J. Simon, O. Zeitler, and I. Carusotto, *ArXiv e-prints* (2018), arXiv:1802.04173 [physics.optics].
- [38] R. El-Ganainy, K. G. Makris, M. Khajavikhan, Z. H. Musslimani, S. Rotter, and D. N. Christodoulides, *Nature Physics* **14**, 11 (2018).
- [39] S. Longhi, *ArXiv e-prints* (2018), arXiv:1802.05025 [physics.optics].
- [40] V. Kozii and L. Fu, *ArXiv e-prints* (2017), arXiv:1708.05841 [cond-mat.mes-hall].
- [41] M. Papaj, H. Isobe, and L. Fu, *ArXiv e-prints* (2018), arXiv:1802.00443 [cond-mat.dis-nn].
- [42] H. Shen and L. Fu, *ArXiv e-prints* (2018), arXiv:1802.03023 [cond-mat.str-el].
- [43] H. Zhou, C. Peng, Y. Yoon, C. W. Hsu, K. A. Nelson, L. Fu, J. D. Joannopoulos, M. Soljačić, and B. Zhen, (2018), 10.1126/science.aap9859.
- [44] H. Shen, B. Zhen, and L. Fu, *Phys. Rev. Lett.* **120**, 146402 (2018).
- [45] K. Esaki, M. Sato, K. Hasebe, and M. Kohmoto, *Phys. Rev. B* **84**, 205128 (2011).
- [46] T. E. Lee, *Phys. Rev. Lett.* **116**, 133903 (2016).
- [47] D. Leykam, K. Y. Bliokh, C. Huang, Y. D. Chong, and F. Nori, *Phys. Rev. Lett.* **118**, 040401 (2017).
- [48] S. Lieu, *Phys. Rev. B* **97**, 045106 (2018).
- [49] Y. Xiong, *ArXiv e-prints* (2017), arXiv:1705.06039v1 [cond-mat.mes-hall].
- [50] V. M. Martinez Alvarez, J. E. Barrios Vargas, and L. E. F. Foa Torres, *Phys. Rev. B* **97**, 121401 (2018).
- [51] Z. Gong, Y. Ashida, K. Kawabata, K. Takasan, S. Higashikawa, and M. Ueda, *ArXiv e-prints* (2018), arXiv:1802.07964v1 [cond-mat.mes-hall].
- [52] S. Yao and Z. Wang, *ArXiv e-prints* (2018), arXiv:1803.01876 [cond-mat.mes-hall].
- [53] M. S. Rudner and L. S. Levitov, *Phys. Rev. Lett.* **102**, 065703 (2009).
- [54] S.-D. Liang and G.-Y. Huang, *Phys. Rev. A* **87**, 012118 (2013).
- [55] Y. C. Hu and T. L. Hughes, *Phys. Rev. B* **84**, 153101 (2011).
- [56] J. Gong and Q.-h. Wang, *Phys. Rev. A* **82**, 012103 (2010).
- [57] M. S. Rudner, M. Levin, and L. S. Levitov, *ArXiv e-prints* (2016), arXiv:1605.07652 [cond-mat.mes-hall].
- [58] B. Zhu, R. Lü, and S. Chen, *Phys. Rev. A* **89**, 062102 (2014).
- [59] Z. Gong, S. Higashikawa, and M. Ueda, *Phys. Rev. Lett.* **118**, 200401 (2017).
- [60] X. Wang, T. Liu, Y. Xiong, and P. Tong, *Phys. Rev. A* **92**, 012116 (2015).
- [61] K. Kawabata, Y. Ashida, H. Katsura, and M. Ueda, *arXiv preprint arXiv:1801.00499* (2018).
- [62] X. Ni, D. Smirnova, A. Poddubny, D. Leykam, Y. Chong, and A. B. Khanikaev, *ArXiv e-prints* (2018), arXiv:1801.04689 [cond-mat.mes-hall].
- [63] A. A. Zyuzin and A. Y. Zyuzin, *Phys. Rev. B* **97**, 041203 (2018).
- [64] A. Cerjan, M. Xiao, L. Yuan, and S. Fan, *Phys. Rev. B* **97**, 075128 (2018).
- [65] M. Klett, H. Cartarius, D. Dast, J. Main, and G. Wunner, *Phys. Rev. A* **95**, 053626 (2017).
- [66] H. Menke and M. M. Hirschmann, *Phys. Rev. B* **95**, 174506 (2017).
- [67] L. Zhou, Q.-h. Wang, H. Wang, and J. Gong, *ArXiv e-prints* (2017), arXiv:1711.10741 [cond-mat.stat-mech].
- [68] J. González and R. A. Molina, *Phys. Rev. B* **96**, 045437 (2017).
- [69] C. Yuce, *Phys. Rev. A* **93**, 062130 (2016).
- [70] W. Hu, H. Wang, P. P. Shum, and Y. D. Chong, *Phys. Rev. B* **95**, 184306 (2017).
- [71] Y. Xu, S.-T. Wang, and L.-M. Duan,

- Phys. Rev. Lett. **118**, 045701 (2017).
- [72] S. Ke, B. Wang, H. Long, K. Wang, and P. Lu, Optics Express **25**, 11132 (2017).
- [73] C. Yin, H. Jiang, L. Li, R. Lü, and S. Chen, ArXiv e-prints (2018), arXiv:1802.04169v1 [cond-mat.mes-hall].
- [74] G. Harari, M. A. Bandres, Y. Lumer, M. C. Rechtsman, Y. Chong, M. Khajavikhan, D. N. Christodoulides, and M. Segev, Science , eaar4003 (2018).
- [75] J. M. Zeuner, M. C. Rechtsman, Y. Plotnik, Y. Lumer, S. Nolte, M. S. Rudner, M. Segev, and A. Szameit, Phys. Rev. Lett. **115**, 040402 (2015).
- [76] L. Xiao, X. Zhan, Z. H. Bian, K. K. Wang, X. Zhang, X. P. Wang, J. Li, K. Mochizuki, D. Kim, N. Kawakami, W. Yi, H. Obuse, B. C. Sanders, and P. Xue, Nature Physics **13**, 1117 (2017).
- [77] S. Weimann, M. Kremer, Y. Plotnik, Y. Lumer, S. Nolte, K. Makris, M. Segev, M. Rechtsman, and A. Szameit, Nature materials **16**, 433 (2017).
- [78] C. Poli, M. Bellec, U. Kuhl, F. Mortessagne, and H. Schomerus, Nature communications **6**, 6710 (2015).
- [79] M. Parto, S. Wittek, H. Hodaei, G. Harari, M. A. Bandres, J. Ren, M. C. Rechtsman, M. Segev, D. N. Christodoulides, and M. Khajavikhan, ArXiv e-prints (2017), arXiv:1709.00523 [physics.optics].
- [80] H. Zhao, P. Miao, M. H. Teimourpour, S. Malzard, R. El-Ganainy, H. Schomerus, and L. Feng, ArXiv e-prints (2017), arXiv:1709.02747 [physics.optics].
- [81] X. Zhan, L. Xiao, Z. Bian, K. Wang, X. Qiu, B. C. Sanders, W. Yi, and P. Xue, Phys. Rev. Lett. **119**, 130501 (2017).
- [82] M. Z. Hasan and C. L. Kane, Rev. Mod. Phys. **82**, 3045 (2010).
- [83] X.-L. Qi and S.-C. Zhang, Rev. Mod. Phys. **83**, 1057 (2011).
- [84] C.-K. Chiu, J. C. Y. Teo, A. P. Schnyder, and S. Ryu, Rev. Mod. Phys. **88**, 035005 (2016).
- [85] B. A. Bernevig and T. L. Hughes, *Topological insulators and topological superconductors* (Princeton University Press, Princeton, NJ, 2013).
- [86] M. A. Bandres, S. Wittek, G. Harari, M. Parto, J. Ren, M. Segev, D. N. Christodoulides, and M. Khajavikhan, Science , eaar4005 (2018).
- [87] X.L. Qi, Y.S. Wu, and S.C. Zhang, Phys. Rev. B **74**, 085308 (2006).
- [88] F. D. M. Haldane, Phys. Rev. Lett. **61**, 2015 (1988).
- [89] T. D. Lee and C. N. Yang, Phys. Rev. **87**, 410 (1952).
- [90] A. Mostafazadeh, Journal of Mathematical Physics **43**, 205 (2002), math-ph/0107001.
- [91] A. Mostafazadeh, Journal of Mathematical Physics **43**, 2814 (2002), math-ph/0110016.
- [92] The gap in $L \rightarrow \infty$ limit is determined from the intercept in the gap^2-1/L^2 plot.
- [93] In the 1D non-Hermitian SSH model, an analogous phenomenon has been seen numerically[50] and analytically[52].